Geomechanics and Engineering, *Vol. 35, No. 4 (2023) 395-409*
https://doi.org/10.12989/gae.2023.35.4.395

Analysis of stability control and the adapted ways for building tunnel anchors and a down-passing tunnel

Xiaohan Zhou[1,2], Xinrong Liu[*1,2], Yu Xiao[3], Ninghui Liang[**1,2], Yangyang Yang[1,2], Yafeng Han[4] and Zhongping Yang[1,2]

[1]*Key Laboratory of New Technology for Construction of Cities in Mountain Area, Ministry of Education, Chongqing University, Chongqing 400045, China*
[2]*School of Civil Engineering, Chongqing University, Chongqing 400045, China*
[3]*Chongqing City Infrastructure Construction LTD, Chongqing 400045, China*
[4]*Chongqing Jiaotong University, Chongqing 400074, China*

(*Received July 9, 2023, Revised October 24, 2023, Accepted November 1, 2023*)

Abstract. Long-span suspension bridges have tunnel anchor systems to maintain stable cables. More investigations are required to determine how closely tunnel excavation beneath the tunnel anchor impacts the stability of the tunnel anchor. In order to investigate the impact of the adjacent tunnel's excavation on the stability of the tunnel anchor, a large-span suspension bridge tunnel anchor is utilised as an example in a three-dimensional numerical simulation approach. In order to explore the deformation control mechanism, orthogonal tests are employed to pinpoint the major impacting elements. The construction of an advanced pipe shed, strengthening the primary support. Moreover, according to the findings the grouting reinforcement of the surrounding rock, have a significant control effect on the settlement of the tunnel vault and plug body. However, reducing the lag distance of the secondary lining does not have such big influence. The greatest way to control tunnel vault settling is to use the grout reinforcement, which increases the bearing capacity and strength of the surrounding rock. This greatly minimizes the size of the tunnel excavation disturbance area. Advanced pipe shed can not only increase the surrounding rock's bearing capacity at the pipe shed, but can also prevent the tunnel vault from connecting with the disturbance area at the bottom of the anchorage tunnel, reduce the range of shear failure area outside the anchorage tunnel, and have the best impact on the plug body's settlement control.

Keywords: construction of adjacent underpass tunnel; numerical simulation; orthogonal experiment; settlement control; stability control measures; tunnel anchor

1. Introduction

With the rapid expansion of domestic traffic construction scale, more and more projects are facing the challenge of crossing existing structures and even collaborative construction (Liu *et al.* 2022). Tunnel excavation activities in crowded urban areas have increased dramatically. More and more projects are facing the problem of crossing existing projects. such as joint construction. When new tunnels are built (Tao *et al.* 2020, Ding *et al.* 2019), the current situation of existing tunnels (Tao *et al.* 2021), above-ground buildings, underground pipelines (Ding *et al.* 2023), large and deep foundation pits and other projects (Shi *et al.* 2023) is gradually increasing.

The issue of neighboring new tunnel building and existing tunnel construction has been raised in studies on the construction of adjacent tunnels (Li *et al.* 2021). For example, a new tunnel passes through one or more existing tunnels to study the safety of new tunnels and existing tunnels (Gong *et al.* 2022, Yoo *et al.* 2020). There are frequently two lines of the tunnel being constructed simultaneously. (Li et al.2022), so the influence of the left line tunnel construction and the right line adjacent tunnel construction on the tunnel structure is studied. Underground engineering also includes municipal tunnels (Lu *et al.* 2012) and underground pipelines (Wang *et al.* 2022). Many scholars use numerical simulation, scaled experiment and other means (Gong *et al.* 2015) to study the safety of the adjacent construction of new tunnels and underground projects (Ding *et al.* 2017). In addition to the engineering research in the stratum, there are also studies related to the safe construction of the adjacent construction of underwater tunnels. For example, the method (Zhou *et al.* 2019) of dividing the influence area of the adjacent construction of underwater tunnels is proposed and applied to the analysis of engineering examples. There are also studies on the impact of ground construction on existing tunnels, such as the impact of deep foundation pit excavation (Guo *et al.* 2018), building construction (Yuan *et al.* 2019) and bridge construction and operation (Wang *et al.* 2013) on the safety of existing tunnels. However, In the research of tunnel nearby construction, relatively there is few studies about the tunnel anchor. The current available researches on tunnel anchor engineering mainly focuses on its construction

*Corresponding author, Ph.D.
E-mail: m13368185903@163.com
**Corresponding author, Ph.D.
E-mail: liangninghui0705@163.com

ISSN: 2005-307X (Print), 2092-6219 (Online)

technology (Shen *et al.* 2022), bearing characteristics (Li *et al.* 2017, Xiong *et al.* 2018, Han *et al.* 2020), deformation and failure (Jiang *et al.* 2021, Seo *et al.* 2021, Liu *et al.* 2020), stability (Zhang *et al.* 2015, Tao *et al.* 2019) and stress changes of surrounding rock (Liu *et al.* 2019). Which means that theer are few studies on the adjacent construction of tunnel anchors. In addition, there is little researches about the influence of the adjacent construction of tunnels under tunnel anchors.

As a result, based on a specific project, this paper investigates four types of stability control measures commonly used in tunnel construction. These types are as the follwoing: adopting advanced pipe shed support, improving the initial support strength, shortening the distance between the tunnel face and the second lining, and surrounding rock grouting reinforcement (Li *et al.* 2013, Wang *et al.* 2022, Li *et al.* 2019, Jin *et al.* 2018, Dong *et al.* 2012). The orthogonal test approach is employed to identify the critical variables and quantify the extent to which these four interventions affect the settlement control impact of the tunnel and anchor plug. The control effect is then investigated to uncover its settlement control mechanism. Therefore, it is of great practical significance to study the influence of tunnel construction on the pull-out mechanical behavior of tunnel anchorage of suspension bridge and the corresponding stability control technology to ensure the safty of the construction and the engineering quality.

2. Engineering situation and establishment of numerical model

2.1 Engineering situation

The Lvzhijiang Bridge is a Yuxi-Chuxiong Expressway control project. It is a 780-m-long steel box girder suspension bridge with a single tower and span. As illustrated in Fig. 1, the anchorages on both sides of the bridge are tunnel anchorages.

The studied tunnel is a two-lane highway multiarch tunnel. The tunnel excavation contour is 25.46 m wide (double holes) and 11.1 m high. The relationship between the lower arch tunnel and the upper anchor plug is shown in Fig. 2. The minimum spacing between the anchor and the tunnel is 32 m. The tunnel anchorage is a large concrete

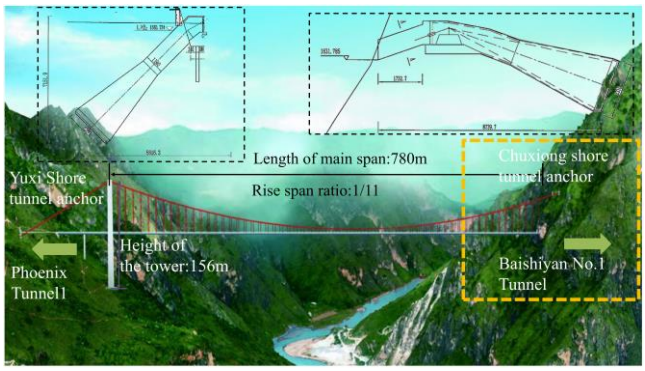

Fig. 1 Structural diagram of Lvzhijiang Bridge

structure. The Baishiyan No. 1 tunnel is also a key control project of the Yuchu Expressway. Therefore, it is necessary to study the mechanical response mechanism of the tunnel anchor under the construction disturbance of the tunnel and the interaction between them during the construction sequence.

The excavation method of a multiarch tunnel adopts the method of a single hole first and an expanding hole later. The CD method is used for construction in a single hole, and the footage of a single step of excavation is 2.5 m. This method is shown in Fig. 3.

First, the upper step I on the right side of the right hole has been excavated, then the initial support for 1 with the temporary support has been applied are applied. After that the lower step II on the right side of the right hole has been excavated., The initial support for 2 with the temporary support B has been installed. After excavating the right hole and installing the initial support, the inverted arch and the secondary lining has been applied. After this step the temporary support A is removed when the secondary lining is applied. The excavation of the left hole has been started.

The first support is installed in its appropriate place. While, the second lining of the left hole is built, the temporary support for B has been taken out. The excavation process causes the construction of the lower step to lag behind the upper step by 2 feet. The single hole temporary initial support within the lower step has been lagged behind the upper step by 6 feet. Moreover, the construction of the left hole to has been lagged behind the construction of the right hole by 36 feet.

2.2 Establishment of the numerical model

In order to assist the development of numerical simulation research (Zhou et al. 2020), the following basic assumptions have been developed for the numerical model. The construction sequence between the tunnel anchor and underpass tunnel have been considered as the following:

- It is assumed that the rock mass, anchor plug body, anchor, and tunnel supporting structure are isotropic homogenous materials.
- It is assumed that the rock mass is a continuous material, without discontinuities, holes, and other flaws.
- It is assumed that the rock merely generates the initial stress field due to gravity without taking into account the influence of the tectonic stress field.
- The effects of precipitation, temperature fluctuation, seepage, groundwater, and other elements have been ignored.
- It is assumed that the anchor-rock contact surface is a thin contact surface element.
- The classical Mohr–Coulomb shear model has been selected as the rock mass constitutive model. While, the elastic linear elastic model has been chosen for the concrete as a constitutive relation.

Figs. 4(a) and 4(b) depicts the model, the shell elements of the anchor and tunnel primary support, as well as the interface elements of the anchor-rock interface, are established in FLAC3D6.0. According to current research, the model size is 180 m × 200 m × 180 m. The tunnel has a

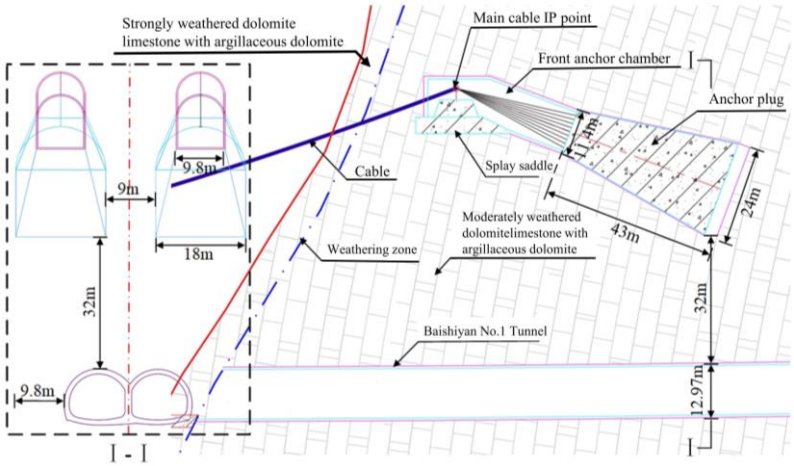

Fig. 2 Positional relationship between the tunnel anchorage and underpass tunnel

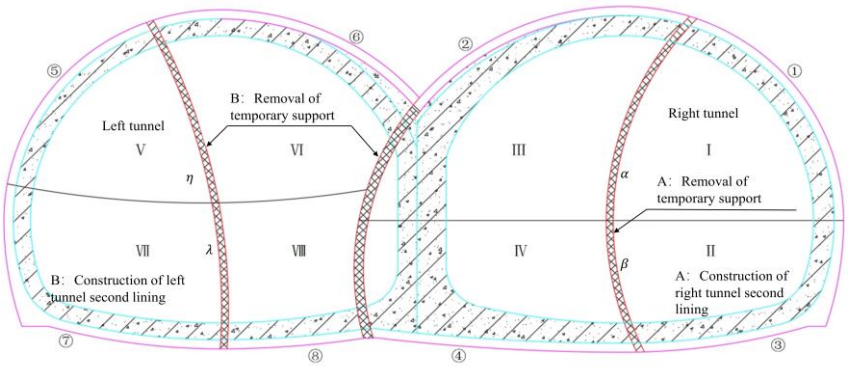

(a) Tunnel construction structure

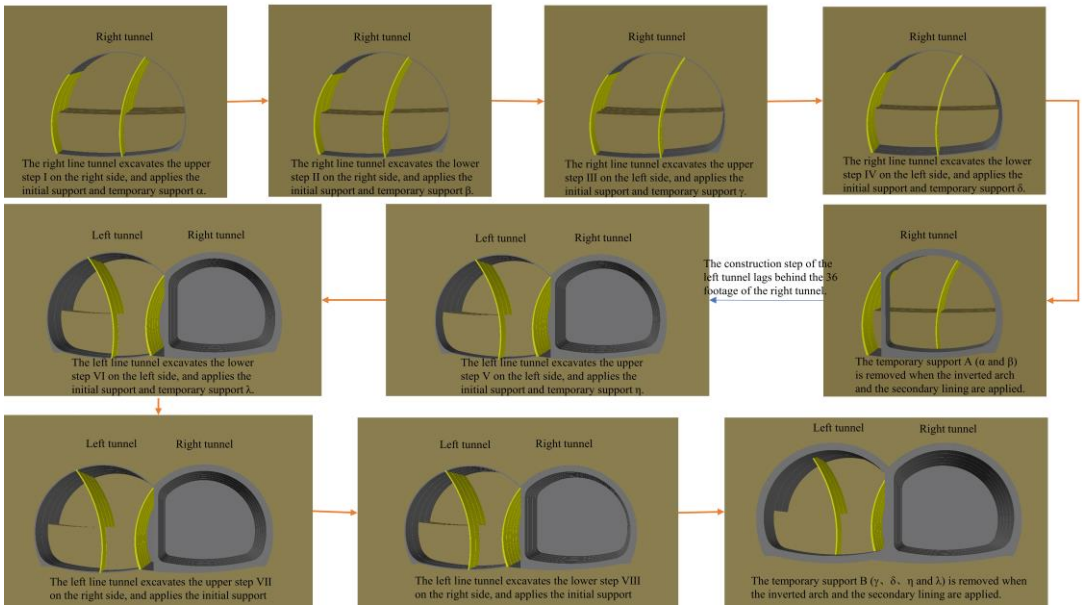

(b) Tunnel construction steps

Fig. 3 depicts the construction procedure

maximum burial depth of 120 m and is 32 m from the bottom of the anchor surface behind the anchor plug. The angle formed by the slope and the horizontal direction is 70°. The model's top and slope surface have free boundaries. Whereas, the left and right sides and back have been normally constraints, and the bottom has a fixed restriction.

Three-dimensional solid elements form the surrounding rock. The tunnel's secondary lining, the front anchor chamber's secondary lining, and the anchor plug body

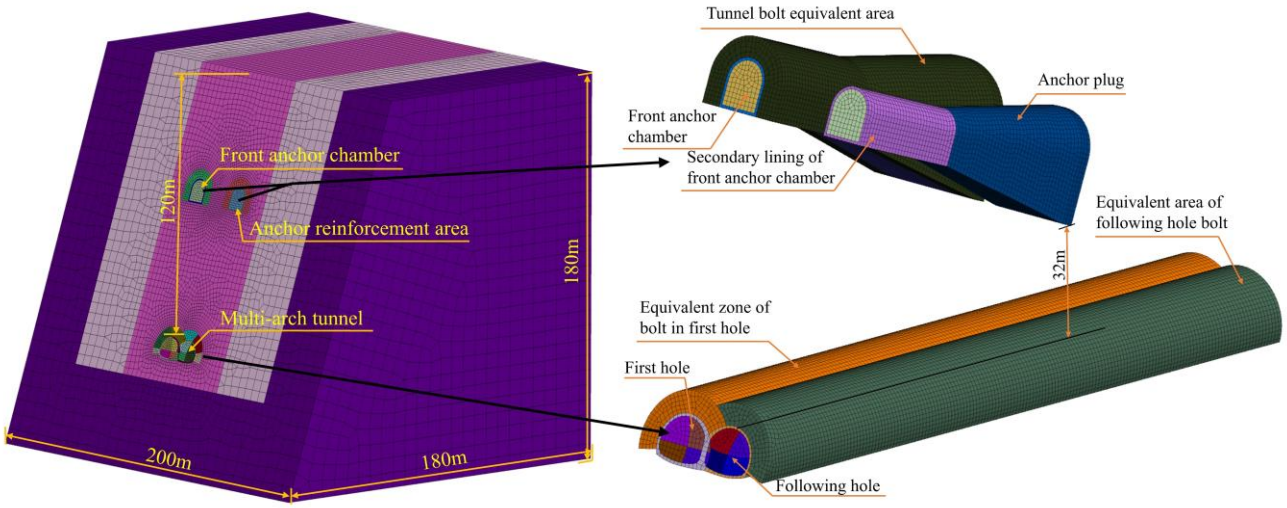

(a) Overview of the numerical model (b) Tunnel anchor and underpass tunnel

Fig. 4 Schematic diagram of the numerical model

(Shahin *et al.* 2016, Liu *et al.* 2017, Ng *et al.* 2004). A three-dimensional solid element of the equivalent reinforcement area is used to simulate the anchor bolt. Shell elements are used to simulate the initial support of the anchor hole. The initial support of the tunnel, and the middle wall of the temporary support of the tunnel CD method. The thickness of the shell element of the tunnel's initial support is 25 cm. The thickness of the secondary lining is 50 cm. The initial support of the anchor hole is 26 cm thick, the secondary lining is 40 cm thick, and the middle partition wall is 137.6 cm thick.

3. Study on the factors influencing settlement

3.1 Purpose of the orthogonal test

Orthogonal testing (Liu *et al.* 2022) is a method for studying multifactor and multilevel relationships. Some representative factors are chosen from the comprehensive test using the orthogonality principle. Underpass tunnel construction will have a greater impact on the upper tunnel anchor, which will be unable to meet the maximum allowable post construction tunnel anchor displacement. Stability control measures for the underpass tunnel is needed. The sensitivity of each control measure is studied by an orthogonal test considering the selection of stability control measures and a large number of full tests.

3.2 Orthogonal experimental design

Under the following conditions: the surrounding rock grade is IV2, the tunnel burial depth is 210 m, and the anchor-tunnel spacing is 20 m, the orthogonal test design has been conducted. Four stability control measures for the advanced pipe shed support, surrounding rock grouting reinforcement, initial support strength improvement, and initial support-secondary lining spacing shortening have been accomplished. Four levels were selected, one level for each one of the four variables. In the numerical simulation, the advanced pipe shed and surrounding rock grouting has been simulated by the equivalent area. As shown in Fig. 5. The grouting equivalent area and the bolt equivalent area are overlapped, and the width is 3.5 m; the equivalent area of the pipe shed is close to the upper boundary of the tunnel with a width of 1.5 m.

The mechanical characteristics of the equivalent area of the pipe shed calculated in the same way as the equivalent area of the anchor rod has been calculated (Yu *et al.* 1983). 150 mm hollow-section steel pipe used in the pipe shed is filled with high-strength cement mortar. The mortar's elastic modulus is 4 GPa. The diffusion radius is 0.75 m, and the surrounding rock porosity is 0.03. The elastic modulus of the pipe shed's equivalent area is 3.34 MPa. Many factors influence the strength of the equivalent area of the grouting, including the elastic modulus of the slurry and the grouting pressure, so it is difficult to estimate it accurately (Zhuang *et al.* 2022).

The amount of grouting used to strengthen surrounding rock is typically between 10% and 30%. As a result, three values for the elastic modulus enhancement has been chosen for simulation: 10%, 20% and 30%. Table 1 shows the orthogonal test factors and levels, whereas Table 2 shows the physical and mechanical characteristics used in the orthogonal test.

The rock dilatancy coefficient has been considered 1.4. The variance analysis of the orthogonal test results is carried out to explore the significance of each factor. A blank column is added to the orthogonal table design to determine the sum of squares of deviations caused by random errors. The standard orthogonal table of L_{16} (5^4) was established (Table 3).

3.3 Analysis of orthogonal array test results

To examine the control effect of the stability measures, the test circumstances are simulated, and the settlement data for each condition are exported. The test results under each level combination are shown in Fig. 6.

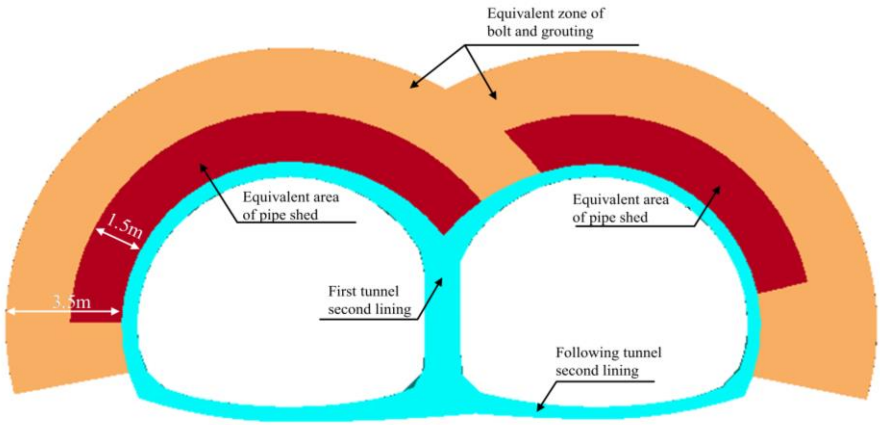

Fig. 5 Schematic diagram of the pipe shed and grouting equivalent area

Table 1 Orthogonal test factors and levels affecting the degree of stability control

Experiment level	Experimental factor			
	Advanced pipe shed construction A	Enhanced initial Support B	Shortened secondary lining lag distance C	Grouted surrounding rock D
1	A_1 No a pipe shed	B_1 C25 sprayed concrete	C_1 Lag distance is 30 m	D_1 No grouting
2	A_2 Length of pipe shed is 5 m	B_2 C30 sprayed concrete	C_2 Lag distance is 25 m	D_2 Elastic modulus increased by 10%
3	A_3 Length of pipe shed is 10 m	B_3 C35 sprayed concrete	C_3 Lag distance is 20 m	D_3 Elastic modulus increased by 20%
4	A_4 Length of pipe shed is 15 m	B_4 C40 sprayed concrete	C_4 Lag distance is 15 m	D_4 Elastic modulus increased by 30%

Table 2 Physical and mechanical parameters used in the orthogonal test

Item	Gravity γ (kN/m^3)	Elastic modulus E (GPa)	Poisson's ratio μ	Internal friction angle φ (°)	Cohesion c (MPa)
Grade IV$_2$ moderately weathered dolomitic limestone	20.5	2.2	0.33	30	0.68
C40 concrete for anchor plugs	25	32.5	0.2	/	/
C30 concrete for secondary lining of front anchor chamber	25	30	0.2	/	/
C25 primary shotcrete for anchor plugs and underpass tunnels	24	26	0.2	/	/
C30 concrete for tunnel secondary lining and middle partition wall	25	30	0.2	/	/
Equivalent region of pipe shed	24	3.34	0.33	30	0.79

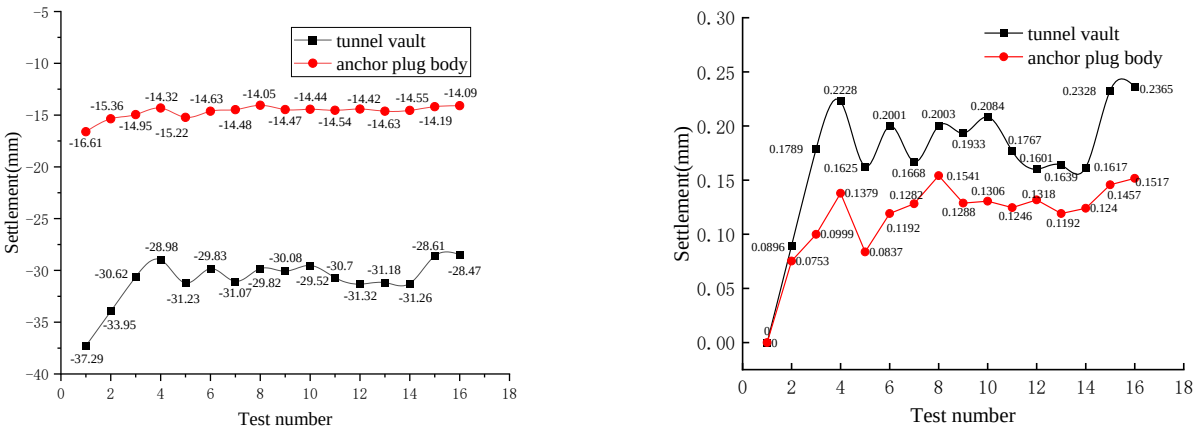

(a)Test result (b) Relative control quantity

Fig. 6 Orthogonal test results

Table 3 $L_{16}(5^4)$ standard orthogonal table (blank column not shown)

Test number	Horizontal combination	Experimental factor			
		Length of advanced pipe shed A	Strength of initial support B	Lag distance of secondary lining C	Elastic modulus of bolt and grouting area D
1	$A_1B_1C_1D_1$	No pipe shed	C25 sprayed concrete	30 m	2.34 MPa
2	$A_1B_2C_2D_2$	No pipe shed	C30 sprayed concrete	25 m	2.57 MPa
3	$A_1B_3C_3D_3$	No pipe shed	C35 sprayed concrete	20 m	2.81 MPa
4	$A_1B_4C_4D_4$	No pipe shed	C40 sprayed concrete	15 m	3.04 MPa
5	$A_2B_1C_2D_3$	The length of the pipe shed is 5 m	C25 sprayed concrete	25 m	2.81 MPa
6	$A_2B_2C_1D_4$	The length of the pipe shed is 5 m	C30 sprayed concrete	30 m	3.04 MPa
7	$A_2B_3C_4D_1$	The length of the pipe shed is 5 m	C35 sprayed concrete	15 m	2.34 MPa
8	$A_2B_4C_3D_2$	The length of the pipe shed is 5 m	C40 sprayed concrete	20 m	2.57 MPa
9	$A_3B_1C_3D_4$	The length of the pipe shed is 10 m	C25 sprayed concrete	20 m	3.04 MPa
10	$A_3B_2C_4D_3$	The length of the pipe shed is 10 m	C30 sprayed concrete	15 m	2.81 MPa
11	$A_3B_3C_1D_2$	The length of the pipe shed is 10 m	C35 sprayed concrete	30 m	2.57 MPa
12	$A_3B_4C_2D_1$	The length of the pipe shed is 10 m	C40 sprayed concrete	25 m	2.34 MPa
13	$A_4B_1C_4D_2$	The length of the pipe shed is 15 m	C25 sprayed concrete	15 m	2.57 MPa
14	$A_4B_2C_3D_1$	The length of the pipe shed is 15 m	C30 sprayed concrete	20 m	2.34 MPa
15	$A_4B_3C_2D_4$	The length of the pipe shed is 15 m	C35 sprayed concrete	25 m	3.04 MPa
16	$A_4B_4C_1D_3$	The length of the pipe shed is 15 m	C40 sprayed concrete	30 m	2.81 MPa

Table 4 Analysis of the range of tunnel vault settlement

Experimental factor (mm)	Advanced pipe shed construction A	Enhanced initial support B	Shortened secondary lining lag distance C	Grouted surrounding rock D	Blank E
R_j	2.830	2.797	1.385	3.360	0.767

3.4 Analysis of tunnel vault settlement

Table 4 shows the range analysis of the orthogonal test based on the settlement of the tunnel vault under 16 working conditions.

Table 4 shows that the four stability control strategies mentioned above have a good control effect on the tunnel vault settlement. When the range change value Rj of tunnel vault settlement induced by different factors is compared, the range of tunnel vault settlement control of factors A, B, C, and D is larger than the range of blank control. The major order of the four control measures on the control effect of tunnel vault settlement are: surrounding rock grouting reinforcement > advanced pipe shed construction > initial support strength enhancement > secondary lining lag distance shortening.

To more correctly estimate the sensitivity of the control effect of tunnel vault settlement to the four stability control measures, the blank case is chosen as the control case under the condition of $\alpha = 0.1$, and the test results are examined using variance analysis (Table 5).

Table 5 Variance analysis of tunnel vault settlement

Experimental factor	Square of deviance	Degree of freedom	F-ratio	F marginal value	Significance
Advanced pipe shed construction A	18.91	3	14.82	5.39	◎
Enhanced primary support strength B	17.73	3	13.89	5.39	◎
Shortened secondary lining lag distance C	5.22	3	4.09	5.39	×
Grouted surrounding rock grouting D	27.34	3	21.43	5.39	◎
Blank E	1.28	3	1		
Error	1.28	3			

Table 5 shows that the grouting reinforcement of the surrounding rock has the most significant controlling effect on tunnel vault settlement. The effect of the two stability

Table 6 Analysis of the range of settlements at the bottom of the plug body

Experimental factor (mm)	Advanced pipe shed construction A	Enhanced initial support B	Shortened secondary lining lag distance C	Grouted surrounding rock D	Blank E
R_j	0.945	0.987	0.500	0.613	0.24

Table 7 Variance analysis of plug body bottom settlement

Experimental factor	Square of deviance	Degree of freedom	F-ratio	F marginal value	Significance
Advanced pipe shed construction A	2.178	3	15.56	5.39	◎
Enhanced primary support strength B	2.071	3	14.79	5.39	◎
Shortened secondary lining lag distance C	0.655	3	4.68	5.39	×
Grouted surrounding rock grouting D	0.756	3	5.40	5.39	○
Blank E	0.140	3	1		
Error	0.14	3			

control measures of the advanced pipe shed and enhanced tunnel primary support on tunnel vault settlement is also significant. The effect of the shortened the secondary lining lag distance is not significant. The conclusion of the variance analysis is consistent with that of the range analysis.

3.5 Analysis of bottom settlement of anchored plug

The range analysis method is also used to study the influence of the control effect of each factor on the settlement at the bottom of the anchor plug under the 16 operating circumstances of the orthogonal test. The settlement at the bottom of the anchor plug calculated from the range analysis is shown in Table 6. Table 6 shows that the four stability control approaches have an obvious control effects on the anchor plug settlement. Tunnel vault settlement control factors A, B, C, and D have a broader range than the blank control. The results of the range analysis of the control factors follow the order of factor B > factor A > factor D > factor C (initial support strength enhancement > advanced pipe shed construction > surrounding rock grouting reinforcement > secondary lining lag distance shortening).

In order to correctly estimate the sensitivity of the four stability control measures to the control effect of the settlement at the bottom of the anchor plug, the blank column was chosen as the control under the condition of $\alpha = 0.1$, and the test results were analysed using variance analysis (Table 7).

Table 7 shows that the advanced pipe shed support and the increased initial support strength have the greatest influences on the bottom settlement of the anchor plug body. F ratio of the control impact of surrounding rock grouting reinforcement on the settlement at the bottom of the anchor plug is 5.40, which is somewhat more than the F test critical threshold of 5.39, suggesting that it has some relevance. The results of variance and range analysis are contradictory. The following four stability control strategies have a substantial impact on the settlement: advanced pipe shed construction > initial support strength enhancement > surrounding rock grouting reinforcement > secondary lining lag distance shortening. The most notable issue is that the effects of the advanced pipe shed and enhanced initial support strength are inconsistent. In the range analysis, the range of the advanced pipe shed factor A is 0.945, and the range of the initial support strength component B is 0.987. The F ratio of factor A of the advanced pipe shed is 15.56 in the analysis of variance, while the F ratio of factor B of the enhanced initial support strength is 14.79. The difference in results generated by the two analysis approaches is modest, indicating that their influences are very similar. However, because the range of the analysis cannot rule out the impact of random mistakes, the significance order is determined by the findings of the analysis of variance.

4. Stability control mechanism of surrounding rock grouting reinforcement

The orthogonal test indicates that the optimum method for controlling tunnel vault settling is by using the grouting reinforcement of the surrounding rock. The stress variation characteristics of the model and the development of the plastic zone are examined to determine the internal causes of the decreasing in vault settling caused by surrounding rock grouting. The same numerical model as in the orthogonal test has been implemented in this section to perform single factor analysis on the grouting measures of the surrounding rock and control the remaining support parameters: no advanced pipe shed support is used, C25 spray mixing is used for the initial support, and the second lining lag distance is limited to 30 m. Tunnel excavation and support are carried out under four conditions by varying the elastic modulus of the surrounding rock in the grouting area: 2.34 MPa (only considering the bolt support), 2.57 MPa (10% of the surrounding rock grouting reinforcement), 2.81 MPa (20% of the surrounding rock grouting reinforcement), and 3.04 MPa (30% of the surrounding rock grouting reinforcement). To investigate the stability control mechanism, the deformation characteristics, mechanical response characteristics, and plastic zone development characteristics during excavation are examined.

4.1 Analysis of the deformation characteristics

The tunnel vault settlement curves of the critical steps of tunnel construction are shown in Fig. 7 for various grouting reinforcement degrees. The investigation demonstrates that

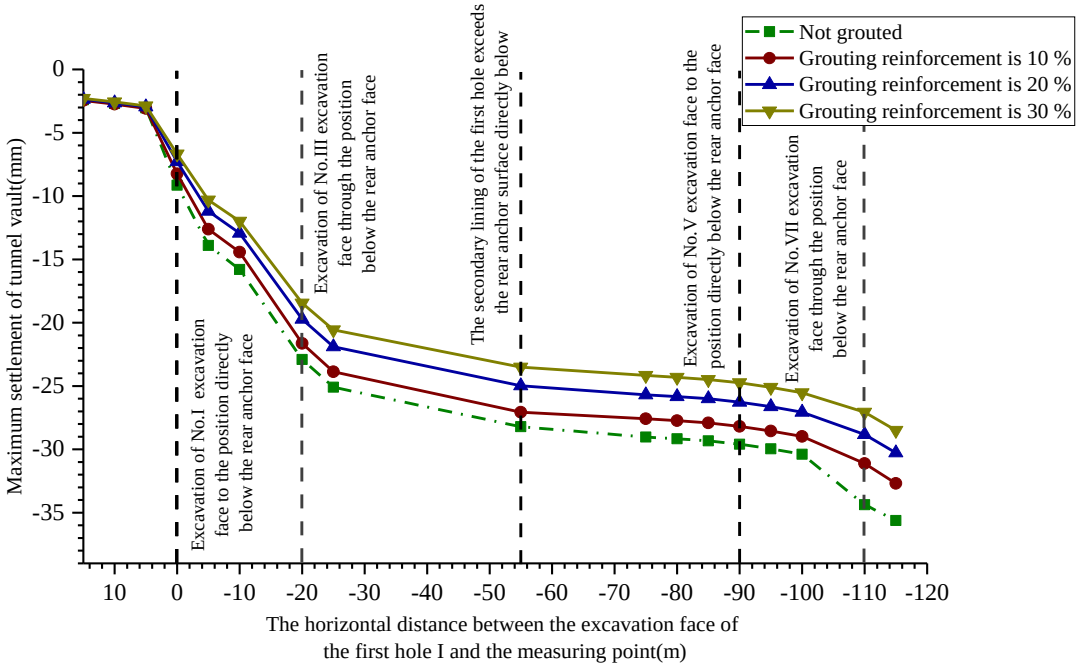

Fig. 7 Settlement curve of the tunnel vault under different grouting reinforcement degrees of the surrounding rock

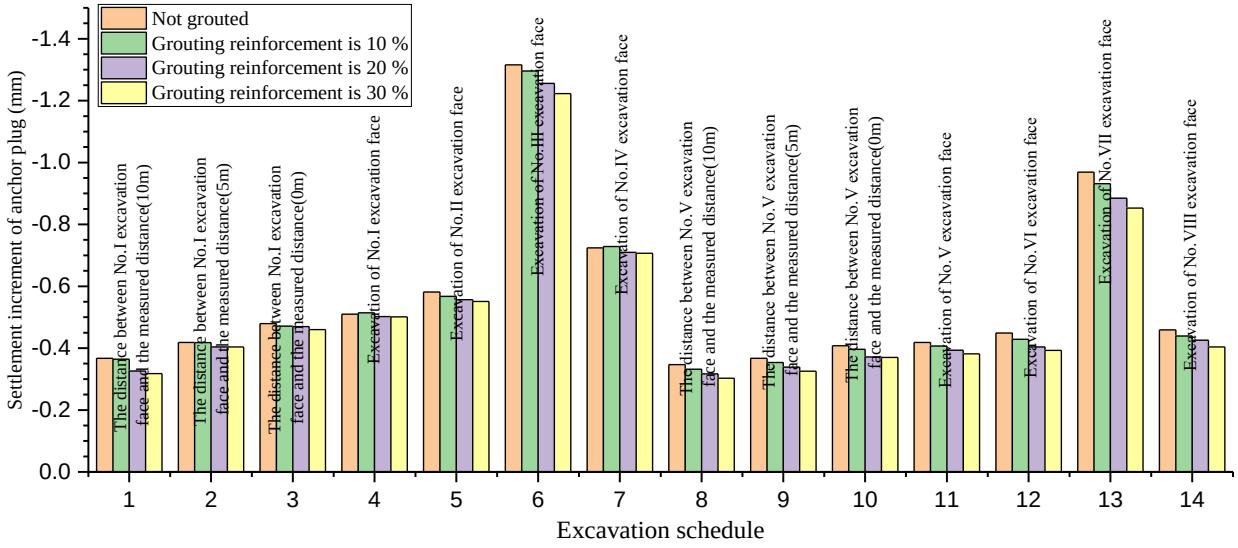

Fig. 8 Settlement increment diagram of the plug body bottom under different grouting reinforcement degrees of the surrounding rock

the surrounding rock grouting has a good control effect on the tunnel vault's settlement. The maximum settlement of the tunnel vault continues to decrease as the grouting reinforcement degree of the surrounding rock improves.

Section 3.5 shows that the grouting reinforcement of the surrounding rock has a good control effect on the settlement of the anchor plug body. Extraction the settlement increment at the bottom of the anchor plug body in an asynchronous sequence can intuitively demonstrate the controlling influence of the surrounding rock grouting on the anchor plug body settlement. The effect of the excavation sequence on the maximum settlement, as shown in Fig. 8, related to the excavation of the No. III face of the first tunnel and the No. VII face of the rear tunnel. The settlement at the bottom of the anchor plug will increase by 1.31 mm and 0.97 mm, respectively, if no grouting reinforcement is used. However, by using the grouting reinforcement of adjacent rock will reduce anchor plug settlement at each excavation stage.

4.2 Analysis of the stress response

The minimal primary stress contour diagram of the monitoring section under varying grouting reinforcement

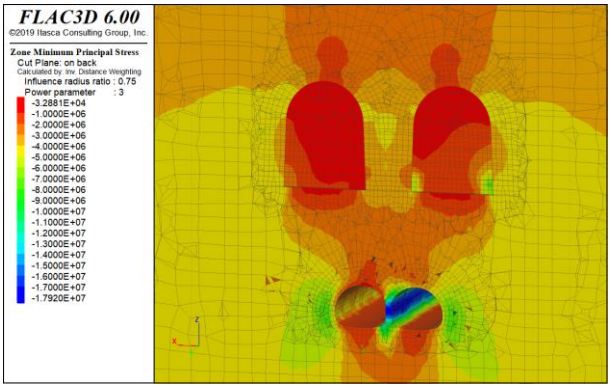

(a) No grouting reinforcement

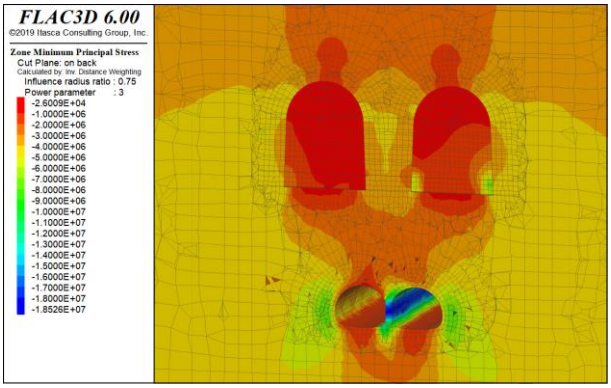

(b) Surrounding rock grouting reinforcement: 10%

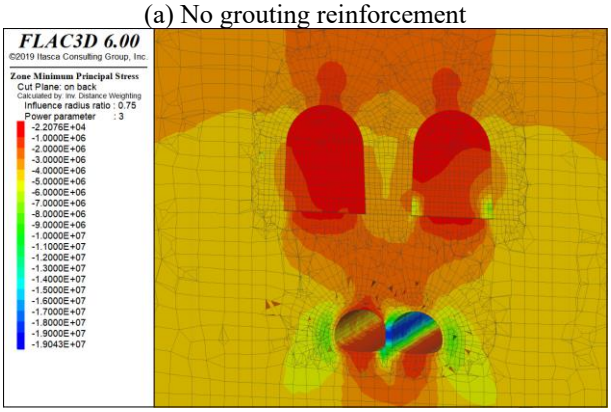

(c) Surrounding rock grouting reinforcement: 20%

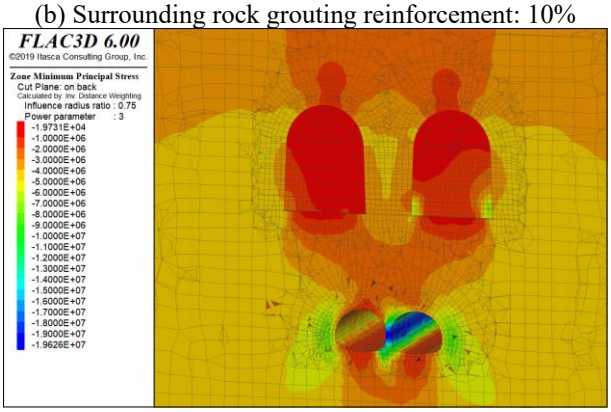

(d) Surrounding rock grouting reinforcement: 30%

Fig. 9 The minimum principal stress contour diagram of the monitoring section under different grouting reinforcement degrees of the surrounding rock

degrees of the surrounding rock is shown in Figs. 9(a)-9(d).

Grouting the surrounding rock has no substantial effect on the spatial distribution characteristics of the monitoring section's minimum principal stress contour diagram, as shown in Figs. 9(a)-9(d). The compressive stress borne by the surrounding rock outside the tunnel haunch is significant, while the compressive stress borne by the surrounding rock between the anchor, the tunnel and the surrounding rock above the anchor hole is modest. The compressive stress borne by the surrounding rock outside the hance of the tunnel steadily increases as the grouting reinforcement of the surrounding rock improves. The compressive stress of the surrounding rock outside the tunnel arch waist without grouting, 10% grouting reinforcement, 20% grouting reinforcement, and 30% grouting reinforcement are -7.04 MPa, -7.66 MPa, -8.16 MPa, and -8.63 MPa, increasing by 8.81%, 15.91%, and 22.59%, respectively. Compressive stress is primarily localized in the central partition wall of the multiarch tunnel from the perspective of the structure. The compressive stress borne by the middle partition wall of a multiarch tunnel increases step by step as the grouting reinforcement degree of the surrounding rock increases, from -17.92 MPa without grouting to -19.63 MPa after 30% grouting reinforcement, a 9.54% increase.

4.3 Analysis of the plastic zone development characteristics

Figs. 10(a)-10(d) depicts the model's plastic zone properties under various grouting reinforcement degrees of the surrounding rock.

According to the growth trend of the plastic zone around the tunnel, as the degree of grouting reinforcement increases, the range of the tensile stress disturbance zone above the rear tunnel gradually decreases. When the surrounding rock grouting reinforcement measures are not used, the tensile stress disturbance zone above the rear tunnel has a height of approximately 12 m and is connected to the superimposed disturbance zone at the bottom of the left anchor plug. The height of the disturbance zone is lowered to 9 m after 10% grouting reinforcement of the surrounding rock, the shape of the superimposed disturbance zone at the bottom of the anchor plug body does not change, and the two disturbance zones are independent of each other. As the degree of grouting reinforcement of the surrounding rock increases, the range of the tunnel vault's disturbance area decreases, and the height decreases. When the surrounding rock grouting reinforcement is 30%, the disturbance region above the back tunnel appears only within approximately 5 m of the vault. Based on the evolution of the plastic zone around the tunnel anchor, it is clear that strengthening the surrounding rock of the undercrossing multiarch tunnel by grouting will not change the shape of the plastic zone near the anchor hole. The surrounding rock outside the anchor hole has a wide range of shear failure zones at all four levels, and the plastic zone shape of the surrounding rock at the top and bottom of the anchor hole is essentially the same.

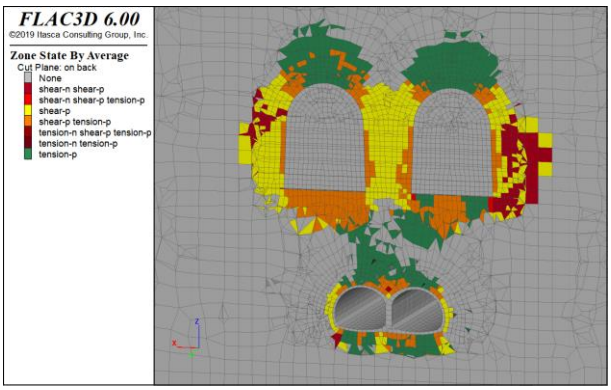

(a) Only considering bolt support

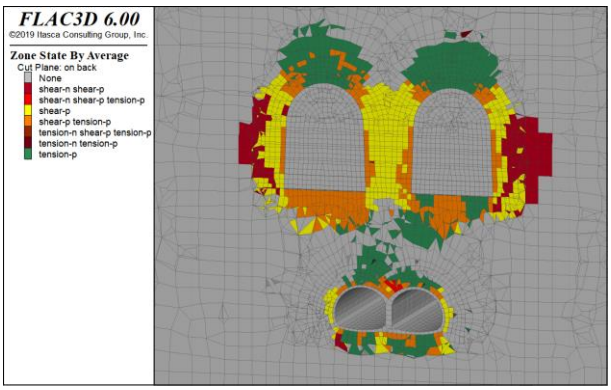

(b) Surrounding rock grouting reinforcement: 10%

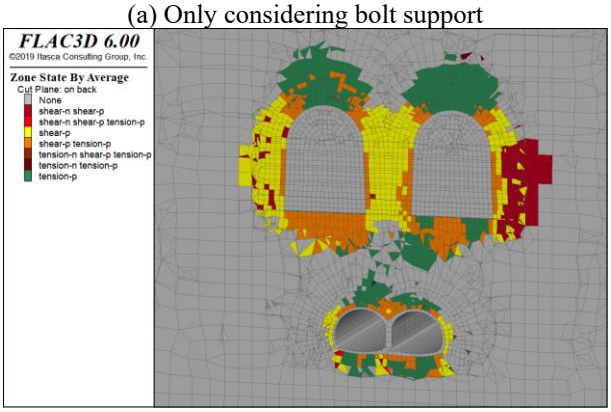

(c) Surrounding rock grouting reinforcement: 20%

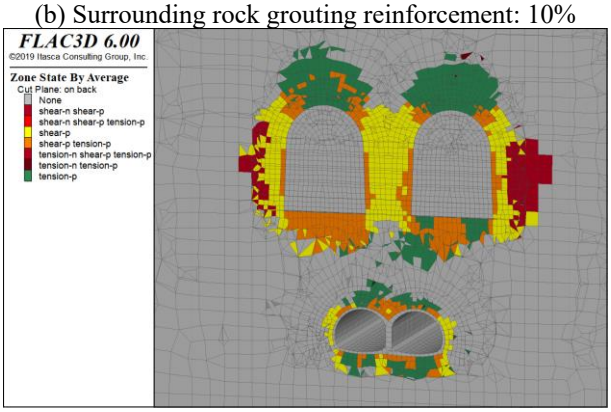

(d) Surrounding rock grouting reinforcement: 30%

Fig. 10 Characteristic diagram of the plastic zone of the monitoring section under different grouting reinforcement degrees of the surrounding rock

5. Stability control mechanism of the advanced pipe shed

The advanced pipe shed has the most significant controlling impact when the anchor plug body's settling which has been chosen as the assessment standard. As a result, this section looks at the advanced pipe shed's stability control system. By analyzing the stress variation properties of the model body and the development of the plastic zone, the causes of the decreasing in tunnel vault settling brought on by the advanced pipe shed are identified. In this section, the advanced pipe shed is evaluated, and the remaining support parameters are controlled, including no grouting reinforcement of nearby rock, C25 shotcrete for initial support, and a secondary lining lag distance cap of 30 m. Tunnel excavation and support are carried out under four different conditions: 5 m, 10 m, and 15 m without the advanced pipe shed. Only the length of the advanced pipe shed is changed. The deformation characteristics, mechanical response characteristics, and plastic zone growth characteristics are investigated to get better understanding about the stability controlling mechanism.

5.1 Analysis of the deformation characteristics

The tunnel vault settlement curve of the major step sequence of tunnel construction for various advanced pipe shed lengths is shown in Fig. 11. According to the investigation, the new advanced pipe shed support provides excellent control of the vault settlement, particularly during the excavation stage of the first tunnel. The installation of a 5 m advanced pipe shed can reduce tunnel vault settlement by 4.42 mm. When the length of the advanced pipe shed is expanded from 5 m to 10 m, the tunnel vault settlement is reduced by only 1.03 mm; when the length of the advanced pipe shed is increased from 10 m to 15 m, the tunnel vault settlement remains almost unchanged. The equivalent area method has been utilized in the numerical simulation to simulate the advanced pipe shed, which increases the strength of the surrounding rock in front of the tunnel face before tunnel construction, reducing the deformation of the surrounding rock in the early stage of excavation. However, the settlement of the surrounding rock 10 m from the tunnel face is only -2 mm; therefore, lengthening of the advanced pipe shed has no discernible influence on tunnel vault settlement.

The settlement increment diagram of the bottom of the anchor plug body at various lengths of the advanced pipe shed is shown in Fig. 12. The improved pipe shed has a substantial impact on the anchor plug body settlement control. The settlement increment of the anchor plug in the excavation of the III and VII tunnel faces under the condition of the 5 m advanced pipe shed is 1.21 mm, 8.33% less than that without the pipe roof and 14.04% less than that with the VII tunnel face. The total settlement of the tunnel anchor is reduced by 11.59% after the building of a 15 m advanced pipe shed.

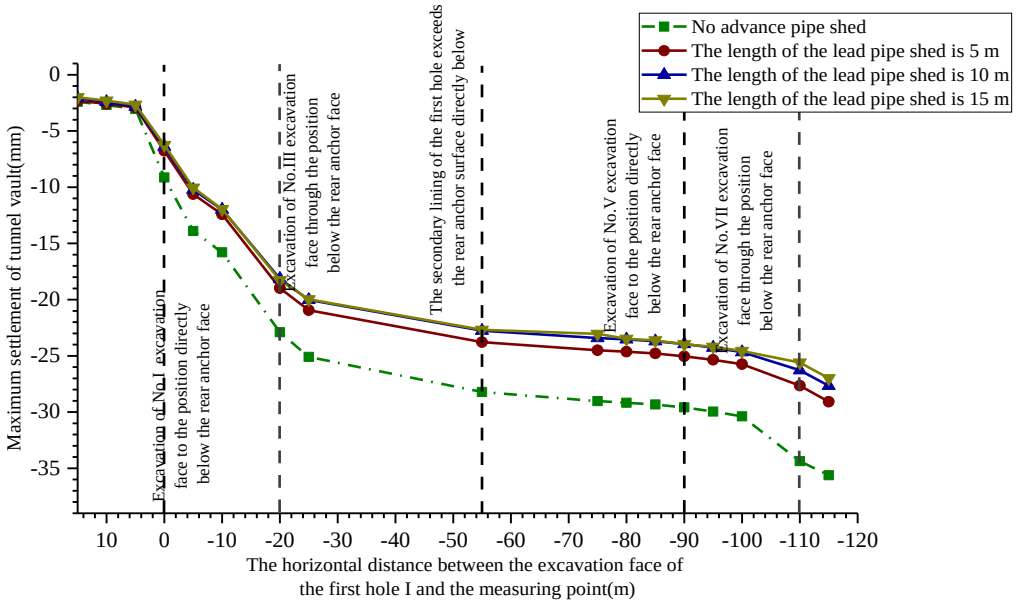

Fig. 11 Settlement curve of the tunnel vault under different advanced pipe shed lengths

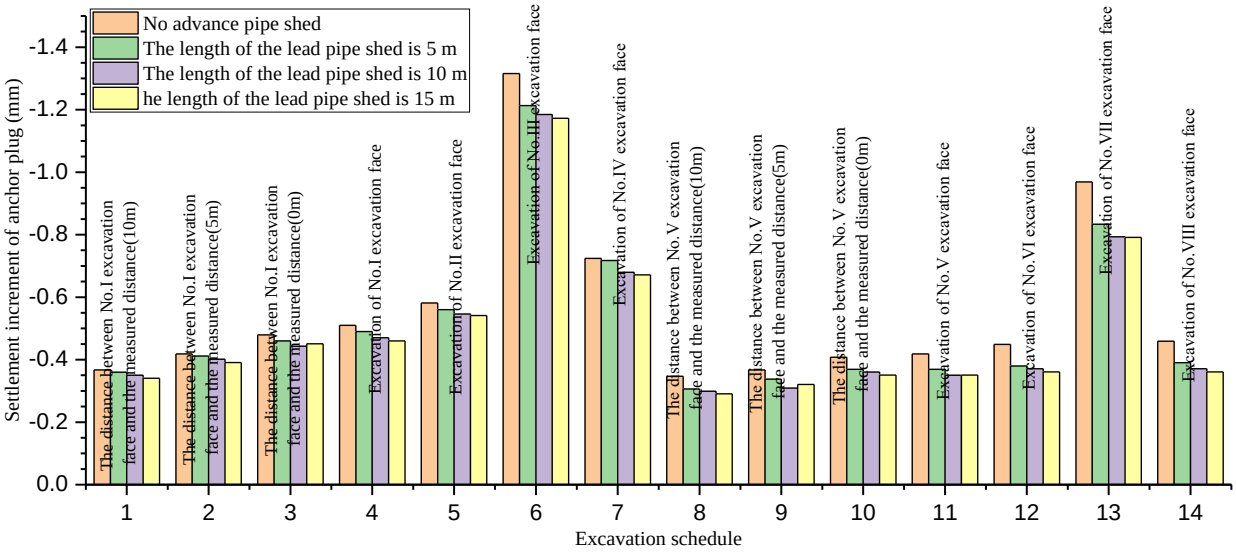

Fig. 12 Settlement increment diagram of plug body bottom under different advanced pipe shed lengths

5.2 Analysis of the stress response characteristics

The stress contour diagram of the No. VII tunnel face excavation via the monitoring section is analysed to investigate the difference between the supporting effect of the advanced pipe shed and the study of other operating conditions. When the No. VIII tunnel face excavation passes through the monitoring section, and the minimum primary stress contour diagram of the monitoring section is shown in Figs. 13(a)-13(d). As shown in Figs. 13(a)-13(d), the use of an advanced pipe shed increases the compressive stress carried by the surrounding rock at the vault in front of the tunnel face. When the advanced pipe shed is not applied, the compressive stress of the surrounding rock at the vault in front of the tunnel face are -1.73 MPa, -1.87 MPa, -2.06 MPa, and -2.30 MPa, respectively when the advanced pipe shed is 5 m, 10 m, and 15 m. The application of an advanced pipe shed, like the grouting reinforcement of the surrounding rock, would increase the compressive stress on the middle partition wall. The compressive load on the middle partition wall, however, only rises from -16.04 MPa to -17.52 MPa due to the small amount of pipe roof.

5.3 Analysis of the plastic zone development characteristics

Figs. 14(a)-14(d) depict the characteristic diagram of the model body's plastic zone at various advanced pipe shed lengths. According to the development trend of the plastic zone around the tunnel, as the length of the advanced pipe

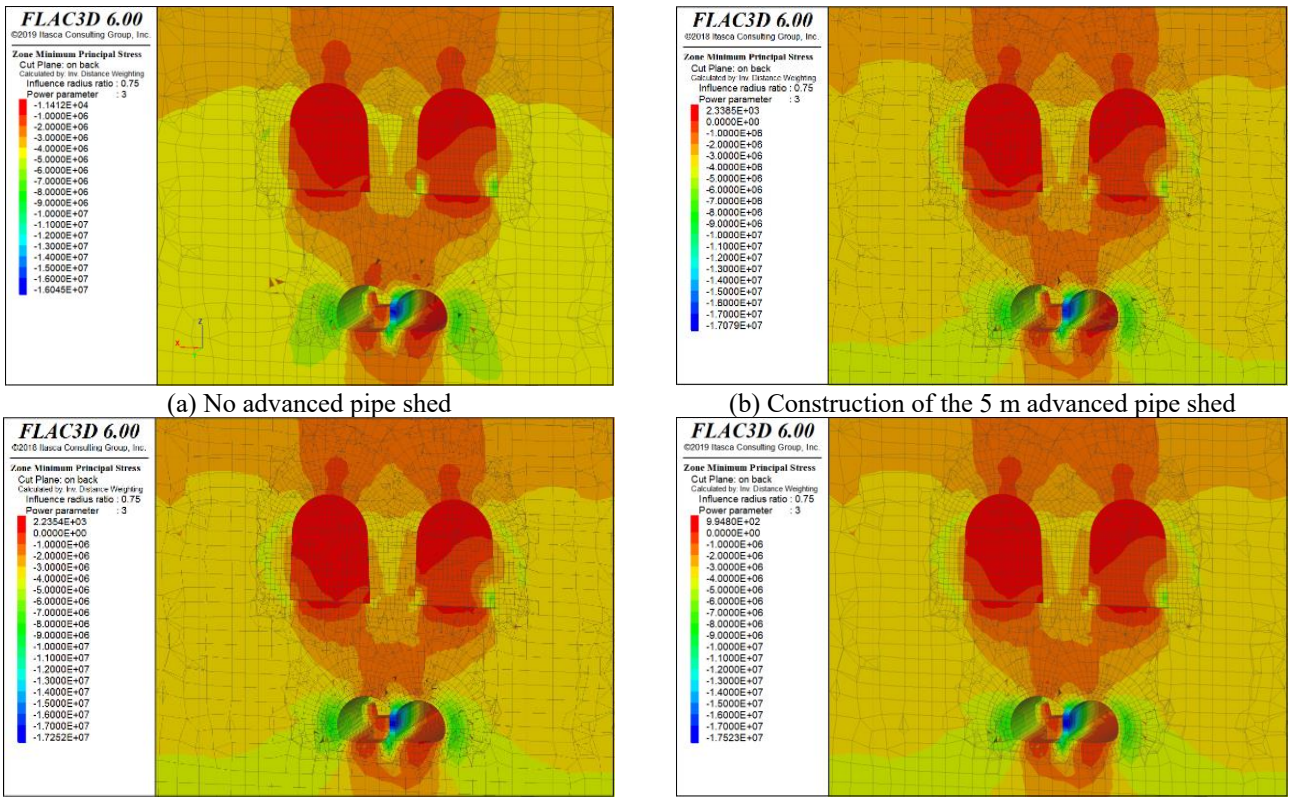

(a) No advanced pipe shed (b) Construction of the 5 m advanced pipe shed

(c) Construction of the 10 m advanced pipe shed (d) Construction of the 15 m advanced pipe shed

Fig. 13 The minimum principal stress contour diagram under different advanced pipe shed lengths

shed increases, the range of the tensile stress disturbance zone above the rear tunnel gradually decreases, but the range and height of the reduction are less than those of the surrounding rock grouting reinforcement. The heights of the disturbance area in a 5 m pipe shed, 10 m pipe shed, and 15 m pipe shed are 10 m, 8 m, and 6 m, respectively. The disturbance zone at the bottom of the anchor hole is independent of the disturbance zone at the tunnel vault due to the building of 10 m long advanced pipe shed. Based on the plastic zone development trend around the tunnel anchor, the use of an advanced pipe shed can reduce the shear failure area of the surrounding rock outside the sidewall of the anchor hole. The failure area of the outer sidewall of the left anchor virtually disappeared after the application of a 15 m pipe roof, while the failure area of the outer sidewall of the right anchor was reduced by approximately 70%.

6. Conclusions

In this paper, the influential degree of these four stability control measures on the settlement control effect of tunnel and anchor plug body is determined by orthogonal experiment. Two key influencing factors have been determined, namely, two measures of surrounding rock grouting reinforcement and advanced pipe shed. Then, the control effect of the two key influential factors was studied, and the settlement control mechanism was explored. The main conclusions are as follows:

- Different control strategies should be employed in different circumstances when tunnel or anchor plug settling is severe. The best way to prevent tunnel vault settling is through grouting reinforcement. The reinforcing measure with the best control impact on the anchor plug body settling is the advanced pipe shed. However, in the treatment of tunnel vault settlement or anchor plug settlement, the new advanced pipe shed has better controlling effect than other treatment methods, indicating that the advanced support has a greater effect on the treatment of tunnel and upper anchor plug settlement.
- The controlling effect of the surrounding rock grouting reinforcement on tunnel vault settlement is obvious. In the case of grouting reinforcement of 10%, 20% and 30%, the proportion of tunnel vault settlement reduction is 8.24%, 15.02% and 20.01% respectively. The principle of controlling settlement is to improve the strength of surrounding rock around the tunnel and improve the bearing capacity of surrounding rock itself, so that the settlement of tunnel vault can be better controlled. However, the control effect of surrounding rock grouting reinforcement on tunnel vault settlement has a certain marginal effect with the improvement of grouting reinforcement degree. At the same time, after grouting reinforcement, the range of tunnel excavation disturbance zone is obviously reduced, which avoids the connection with the disturbance zone at the bottom of the anchor hole, Thus, that more surrounding rock retains its bearing capacity. Reducing the scope of the disturbance zone

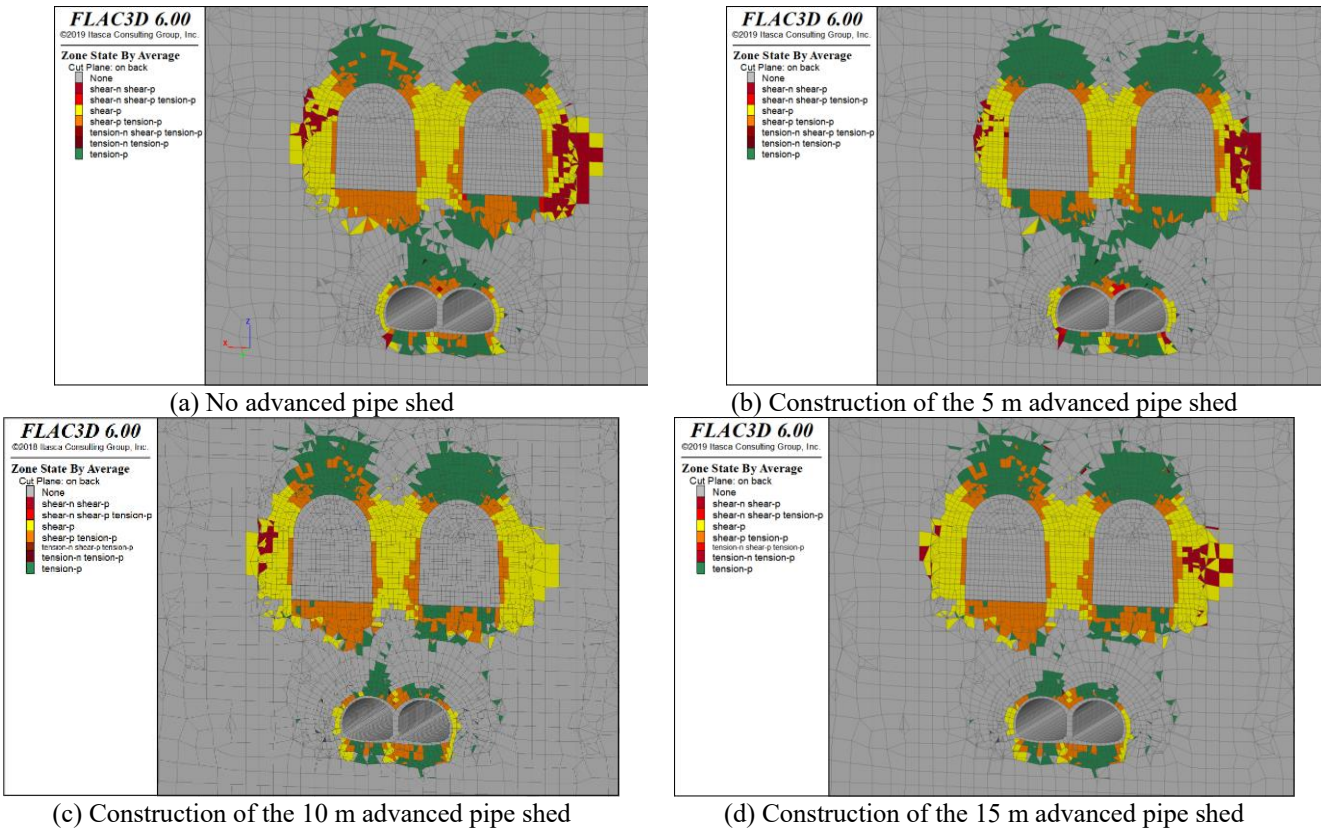

(a) No advanced pipe shed (b) Construction of the 5 m advanced pipe shed

(c) Construction of the 10 m advanced pipe shed (d) Construction of the 15 m advanced pipe shed

Fig. 14 Characteristic diagram of the plastic zone of the monitoring section under different advanced pipe shed lengths

with playing a certain role in controlling the settlement of the anchor plug. After 30 % grouting reinforcement, the total settlement of the anchor plug is reduced by 8.37 %.

- The most evident control impact of advanced pipe shed support on tunnel vault settling. The installation of a 5 m advanced pipe shed can contribute in decreasing the tunnel vault settling by 4.42 mm, especially during the initial tunnel's excavation phase. However, the settling of the tunnel vault is only decreased by 1.03mm when the length of the advance pipe shed is increased from 5m to 10m. By strengthening the rock above the vault and the unexcavated portion, the advance pipe shed also decreases the settling of the tunnel vault. After the advanced pipe shed was built, the height of the disturbance zone during tunnel excavation was also significantly reduced, which prevented a connection with the disturbance zone at the bottom of the anchor hole and had a clear controlling effect on the anchor plug's settlement

Acknowledgments

The study is supported by National Natural Science Foundation of China (Grant No. 41772319, 41972266) and Graduate Scientific Research and Innovation Foundation of Chongqing, China (Grant No. CYB20031). The authors gratefully acknowledge these supports.

References

Ding, P., Shi, C., Tao, L.J., Liu, Z.G. and Zhang, T. (2023), "Research on seismic analysis methods of large and complex underground pipe structures in hard rock sites", *Tunn. Undergr. Sp. Tech. Incorporat. Trenchless Tech. Res.*, **135**. https://doi.org/10.1016/J.TUST.2023.105035.

Ding, P., Tao, L.J., Yang, X.R., Zhao, J. and Shi, C. (2019), "Three-dimensional dynamic response analysis of a single-ring structure in a prefabricated subway station", *Sustain. Cities Soc.*, **45**. https://doi.org/10.1016/j.scs.2018.11.010.

Ding, Z., Wei, X.J. and Wei, G. (2017), "Prediction methods on tunnel-excavation induced surface settlement around adjacent building", *Geomech. Eng.*, **12**(2), 185-195. https://doi.org/12989/gae.2017.12.2.185.

Dong, Q., Wan, H.Y., Kong, F.L. and Zhao, B.Y. (2012), "The 3D numerical simulation and settlement control study for city tunnel crossing high fill geological area of gravelly soils", *Appl. Mech. Mater.*, 1235-1242. https://doi.org/10.4028/WWW.SCIENTIFIC.NET/AMM.256-259.1235.

Gong, J.W., Wang, X. and Sheng, H. (2015), "Numerical analysis on influence of underground space construction on adjacent tunnel", *International Conference on Advances in Energy, Environment and Chemical Engineering, Atlantis Press*, 592-595. https://doi.org/ 10.2991/AEECE-15.2015.118.

Gong, L., Yu, J.W., Sun, X.F., Zhang, Z.X. and Wu, J.L. (2020), "Study on the optimization of the approaching construction of the four-hole large-section municipal tunnels crossing railway tunnel", Research Report No.741; IOP Conference Series: Materials Science and Engineering.

Guo, H.F., Yao, A.J., Zhang, J.T., Zhou, Y.J. and Guo, Y.F. (2018), "Impact of high-rise buildings construction process on adjacent

tunnels", *Adv. Civil Eng*., 2018. https://doi.org/10.1155/2018/5804051.

Han, Y.F., Liu, X.R., Li, D.L., Tu, Y.L., Deng, Z.Y., Liu, D.S. and Wu, X.C. (2020), "Model test on the bearing behaviors of the tunnel-type anchorage in soft rock with underlying weak interlayers", *Bull. Eng. Geol. Environ*., **79**, 1023-1040. https://doi.org/10.1007/s10064-019-01564-5.

Jiang, N., Wang, D., Feng, J., Zhang, S.L. and Huang, L. (2021), "Bearing mechanism of a tunnel-type anchorage in a railway suspension bridge", *J. Mountain Sci*., **18**(8), 2143-2158. https://doi.org/10.1007/S11629-020-6162-8.

Jin, D.L., Yuan, D.J., Li, X.G. and Zheng, H.T. (2018), "An in-tunnel grouting protection method for excavating twin tunnels beneath an existing tunnel", *Tunn. Undergr. Sp. Tech*., **71**, 27-35. https://doi.org/10.1016/j.tust.2017.08.002.

Li, J.J., Bai, H.R. and Li, J.K. (2013), "Analysis and control the surface settlement of tunnel excavation", *Appl. Mech. Mater*., 939-942. https://doi.org/10.4028/www.scientific.net/AMM.438-439.939.

Li, L.D., Liu, D.K., Zhen, Y.H. and Liu, Z.X. (2019), "Force and deformation mechanism of great pipe shed advanced support in subway tunnel", Research Report No.330; IOP Conference Series: Earth and Environmental Science.

Li, P.N., Dai, Z.Y., Huang, D.Z., Cai, W.J. and Fang, T. (2021), "Impact analysis for safety prevention and control of special-shaped shield construction closely crossing multiple operational metro tunnels in shallow overburden", *Geotech. Geol. Eng*., **40**(4). https://doi.org/10.1007/S10706-021-02016-2.

Li, X.H., Qiao, G.L. and Guan, J.W. (2022), "DLSM simulation analysis of the influence of blasting construction on adjacent tunnels in rock mass with discontinuities", *Adv. Civil Engg*., 2022. https://doi.org/10.1155/2022/2214008.

Li, Y.J., Luo, R., Zhang, Q.H., Xiao, G.Q., Zhou, L.M. and Zhang, Y.T. (2017), "Model test and numerical simulation on the bearing mechanism of tunnel-type anchorage", *Geomech. Eng*., **12**(1), 139-160. https://doi.org/10.12989/gae.2017.12.1.139.

Liu, B., Zhang, D.W., Liu, S.Y. and Qin, Y.J. (2017), "Numerical simulation and field monitoring on a large cross-section pipe-jacking underpass traversing existing metro tunnels", *Chinese J. Rock Mech. Eng*., **36**(11), 2850-2860. https://doi.org/10.13722/j.cnki.jrme.2017.1214.

Liu, X.R., Han, Y.F., Li, D.L., Tu, Y.L., Deng, Z.Y., Yu, C.T. and Wu, X.C. (2019), "Anti-pull mechanisms and weak interlayer parameter sensitivity analysis of tunnel-type anchorages in soft rock with underlying weak interlayers", *Eng. Geol*., **253**, 123-136. https://doi.org/10.1016/j.enggeo.2019.03.012.

Liu, X.R., Han, Y.F., Yu, C.T., Xiong, F., Zhou, X.H. and Deng, Z.Y. (2020), "Reliability assessment on stability of tunnel-type anchorages", *Comput. Geotech*., **125**, 103-661. https://doi.org/10.1016/j.compgeo.2020.103661.

Liu, X.R., Zhuang, Y., Zhou, X.H., Li, C., Lin, B.B., Liang, N.H., Zhong, Z.L. and Deng, Z.Y. (2023), "Numerical study of the mechanical process of long-distance replacement of the definitive lining in severely damaged highway tunnels", *Undergr. Sp*., 9. https://doi.org/10.1016/J.UNDSP.2022.07.007.

Lu, JF., Jia, Y.Y. and Liu, B.X. (2012), "Impact of orthogonal undercrossing newly-built tunnel adjacent construction on the safety of existing municipal tunnel", *Disaster Advances*., **5**(4), 756-761.

Ng, C.W.W., Lee, K.M. and Tang, D.K.W. (2004), "Three-dimensional numerical investigations of new Austrian tunnelling method (NATM) twin tunnel interactions", *Can. Geotech. J*., **41**(3), 523-539. https://doi.org/10.1139/t04-008.

Seo S., Lim H. and Chung M. (2021), "Evaluation of failure mode of tunnel-type anchorage for a suspension bridge via scaled model tests and image processing", *Geomech. Eng*., **24**(5), 457-470. https://doi.org/10.12989/gae.2021.24.5.457.

Shahin, H.M., Nakai, T., Ishii, K., Iwata, T. and Kuroi, S. (2016), "Investigation of influence of tunneling on existing building and tunnel: model tests and numerical simulations", *Acta Geotechnica*., **11**, 679-692. https://doi.org/10.1007/s11440-015-0428-2.

Shen, Z.J., Jia, J.H., Jiang, N., Zhu, B. and Sun, W.C. (2022), "Field-scale experiment on deformation characteristics and bearing capacity of tunnel-type anchorage of suspension bridge", *Energies*., **15**(13), 4772. https://doi.org/10.3390/EN15134772.

Shi, C., Tao, L.J., Ding, P., Wang, Z.G. and Jia, Z.B. (2023), "Study on seismic response characteristics and failure mechanism of giant-span flat cavern", *Tunn. Undergr. Sp. Tech. Incorporat. Trenchless Tech. Res*., 140. https://doi.org/10.1016/J.TUST.2023.105328.

Tao, L.J., Ding, P., Lin, H., Wang, H.l., Kou, W.f. and Shi, C. (2021), "Three-dimensional seismic performance analysis of large and complex underground pipe trench structure", *Soil Dynam. Earthq. Eng*., 150. https://doi.org/10.1016/J.SOILDYN.2021.106904.

Tao, L.J., Ding, P., Shi, C., Wu, X.W., Wu, S. and Li, S.C. (2019), "Shaking table test on seismic response characteristics of prefabricated subway station structure", *Tunn. Undergr. Sp. Tech. Incorporat. Trenchless Tech. Res*., https://doi.org/10.1016/j.tust.2019.102994.

Tao, L.J., Ding, P., Yang, X.R., Ling, P., Shi, C., Bao, Y., Wei, P.C. and Zhao, J. (2020), "Comparative study of the seismic performance of prefabricated and cast-in-place subway station structures by shaking table test", *Tunn. Undergr. Sp. Tech. Incorporat. Trenchless Tech. Res*., https://doi.org/10.1016/j.tust.2020.103583.

Wang J.X., Cao A.S., Wu Z., Sun ZP., Lin X., Sun L., Liu X.T., Li H.B.Q. and Sun Y.W. (2022), "Numerical simulation on the response of adjacent underground pipelines to super shallow buried large span double-arch tunnel excavation", *Applied Sciences*., **12**(2), 621. https://doi.org/10.3390/APP12020621.

Wang, T., Wang, L. and Li ,C.N. (2013), "The influence of bridge construction and operation on adjacent Nanjing Yangtze River Tunnels", *Adv. Mater. Res*., 1018-1023. https://doi.org/10.4028/WWW.SCIENTIFIC.NET/AMR.838-841.1018.

Wang, X.L., Li, R.W., Liu, Z.W., Jiang, D.P. and Ji, Z.G. (2022), "Comprehensive evaluation of the reinforcement effect of grouting in broken surrounding rock in deep roadways", *Geotech. Geol. Eng*., 1-12. https://doi.org/10.1007/S10706-021-02037-X.

Xiong, X.R., Tang, H., Liao, M.J., Yin, X.T. and Wang, D.Y. (2018), "Laboratory model test on "wedge-effect" of pullout capacity of tunnel-type anchorage", *Rock Soil Mech*., **39**, 181-190. https://doi.org/10.16285/j.rsm.2018.0405.

Yoo, C. and Cui, S.S. (2020), "Effect of new tunnel construction on structural performance of existing tunnel lining", *Geomech. Eng*., **22**(6), 497-507. https://doi.org/10.12989/gae.2020.22.6.497.

Yu, X.F., Zheng, Y.R., Liu, H.H. and Fang, Z.C. (1983), "Stability analysis of surrounding rock of underground engineering", *Beijing: China Coal*., 1983. (in Chinese).

Yuan, C.F., Yu, H.J., Yuan, Z.J. and Wang, Y.T. (2019), "Numerical simulation of impact caused by construction of high-rise building upon adjacent tunnels", *Geotech. Geol. Eng*., **37**, 3171-3181. https://doi.org/10.1007/s10706-019-00834-z.

Zhang, Q.H., Li, Y.J., Yu, M.W., Hu, H.H. and Hu, J.H. (2015), "Study of the rock foundation stability of the Aizhai suspension bridge over a deep canyon area in China", *Eng. Geol*., **198**, 65-77. https://doi.org/10.1016/j.enggeo.2015.09.012.

Zhou, Z., Chen, Y., Liu, Z.Z. and Miao, L.W. (2020), "Theoretical prediction model for deformations caused by construction of

new tunnels undercrossing existing tunnels based on the equivalent layered method", *Comput. Geotech*., **123**, 103565. https://doi.org/10.1016/j.compgeo.2020.103565.

Zhou, Z., Gao, W.Y., Liu, Z.Z. and, Zhang C.C. (2019), "Influence zone division and risk assessment of underwater tunnel adjacent constructions", *Math. Probl. Eng*., 2019. https://doi.org/10.1155/2019/1269064.

Zhuang, Y., Liu, X.R., Zhou, X.H. and Du, L.B. (2022), "Diffusion model of sulfate ions in concrete based on pore change of cement mortar and its application in mesoscopic numerical simulation", *Struct. Concrete*., **23**(6). https://doi.org/10.1002/SUCO.202100760.

GC